PAPER

Switchable spiral Josephson junction: a superconducting spin-valve proposal

IOP Publishing Superconductor Science and Technology
Supercond. Sci. Technol. **35** (2022) 025002 (10pp) https://doi.org/10.1088/1361-6668/ac3f9f

Switchable spiral Josephson junction: a superconducting spin-valve proposal

N G Pugach[1,*], D M Heim[2], D V Seleznev[1], A I Chernov[3,4,5] and D Menzel[6]

[1] HSE University, Moscow 101000, Russia
[2] Fraunhofer Institute for Industrial Mathematics (ITWM), 67663 Kaiserslautern, Germany
[3] Center for Photonics and 2D Materials, Moscow Institute of Physics and Technology, National Research University, Dolgoprudny 141700, Russia
[4] Russian Quantum Center, Skolkovo Innovation City, Moscow 121353, Russia
[5] V.I. Vernadsky Crimean Federal University, Vernadsky Prospekt, 4, Simferopol 295007, Crimea
[6] Institut für Physik der Kondensierten Materie, Technische Universität Braunschweig, 38106 Braunschweig, Germany

E-mail: npugach@hse.ru

Received 5 September 2021, revised 22 November 2021
Accepted for publication 2 December 2021
Published 29 December 2021

Abstract

We propose a superconducting spin valve based on a Josephson junction with B20-family magnetic metal as a barrier material. Our analysis shows that the states of this element can be switched by reorienting the intrinsic non-collinear magnetization of the spiral magnet. This reorientation modifies long-range spin-triplet correlations and thereby strongly influences the critical Josephson current. Compared to superconducting spin valves proposed earlier, our device has the following advantages: (a) it contains only one barrier layer, which makes it easier to fabricate and control; (b) its ground state is stable, which prevents uncontrolled switching; (c) it is compatible with devices of low-T Josephson electronics. This device may switch between two logical states which exhibit two different values of critical current, or its positive and negative values. I.e. 0-π switch is achievable on a simple Josephson junction.

Keywords: electronic, switchable, spiral, Josephson, junction, superconducting spin valves

(Some figures may appear in colour only in the online journal)

1. Introduction

The urgent need for low-power computing facilities has put a lot of focus on the development of the next generation of superconducting computers [1–4]. In particular, there is a strong need for novel designs of small and effective superconducting memory elements [5, 6]. To meet this demand, we propose a superconducting memory element, which shows certain advantages compared to earlier proposed devices.

Current semiconductor-based computing facilities require large amounts of electricity for operation and cooling purposes [1, 2]. Due to the growing demand for data processing, the search for a low-power solution has gained high priority [3, 7]. Superconducting logical devices are promising alternatives to semiconductor-based ones, because they offer the possibility to exchange information with extreme low energy loss over zero-resistance conductors. However, it is a non-trivial task to design suitable memory elements, which operate effectively at low temperatures and can be miniaturized [5, 6].

Early proposals for superconducting memory elements based on SQUIDs [8, 9] had a relatively large size. Their successors combined SQUIDs with conventional CMOS technology [10, 11] which is better miniaturizable but has a higher energy consumption. The next idea was to use Josephson devices including magnetic interlayers [12–16] which promise a considerable reduction of the element size while staying energy efficient. This idea led to many different proposals e.g. based on φ junctions [17–19], external-field support [20],

* Author to whom any correspondence should be addressed.

triplet-superconductivity [21–23], spin-valves [24–26], spin torque [27], Abrikosov vortices [28], phase domains [29] and nanowires [30].

All these proposals are quite advanced, but also suffer from disadvantages like a difficult fabrication procedure due to a complex design or unstable ground state. In this respect, a superconducting spin valve (SSV) based on a Josephson junction with a single magnetic layer (M) between the superconducting electrodes (S) holds a great promise for applications. A crucial requirement for this type of SSVs is the implementation of magnetic materials with noncollinear magnetic configurations that can be switched with a weak magnetic field. Therefore, itinerant cubic helimagnets of B20 family [31] like MnSi are suitable candidates. B20 family nanomaterials were already proposed to use in a spin valve configuration [23, 32], where the critical temperature T_c changes with the change of the spiral vector direction, possible in B20 family crystals. In recent years, transition metal silicides and germanides being members of the chiral B20 magnets has become a topic of prime interest both for basic research and from the perspective of possible applications. A key characteristic of these compounds is a lack of inversion symmetry with respect to the magnetic ions which gives rise to the antisymmetric Dzyaloshinski-Moriya interaction. In combination with ferromagnetic exchange and magnetocrystalline anisotropy, the B20 magnets exhibit a variety of spin structures starting from spin helices at low external magnetic fields. In MnSi weak crystal-field effects point the helix propagation vector along the $<111>$ directions of the cubic unit cell [33], whereas in $Fe_{1-x}Co_xSi$ the helix vector tends to orient along $<100>$ [34]. For larger fields, the helix vector is unpinned from the equilibrium direction and aligns parallel to the magnetic field resulting in a conical spin state, which completely transforms into a collinear spin alignment in the high field regime [35]. In the vicinity of the ordering temperature a topological spin structure occurs which is referred to as a skyrmion lattice. In MnSi and $Fe_{1-x}Co_xSi$ two-dimensional skyrmions are observed in a small pocket of the H-T-diagram, whereas three-dimensional skyrmions are present in MnGe and $Mn_{1-x}Fe_xGe$ most likely due to enhanced spin–orbit coupling [36].

The occurrence of skyrmionic spin textures holds the prospect of being used for new types of data storage and spintronic devices.

In this work we introduce a SSV based on a Josephson junction with a single magnetic layer. An essential feature of our spin valve is the presence of magnetic order which is characterized by magnetic moments aligned in a spiral around a spiral vector **Q**. This noncollinear magnetic configuration can be switched under the control of a weak parallel magnetic field of circa 100 mT for MnSi [35], which is still much less than the second critical field of Nb electrodes in such Josephson junctions. The magnetic field switch off returns the MnSi film to the initial spiral magnetic state, in a contrast to Er or Ho [37, 38]. We consider the change of the critical current density j_c with the change of the magnetization from the spiral to the uniform one.

This work was also motivated by experiments with thin films of Ho and Er [37, 38] in the MS bilayers. It was shown that the switch of the magnetic configuration from the spiral to uniform turns out the change of the critical temperature of the proximate thin superconducting film. Although helimagnetic metals Ho and Er are not the best choice because being partially magnetized they return in the ground state only at annealing above the Neel temperature, which is higher than the superconducting critical temperature. This fact makes them difficult to use in superconducting nanoelectronic devices.

The j_c changes with the transformation of the magnetic order from the spiral antiferromagnetic to the ferromagnetic one because the non-collinear magnetic moments originating from the spiral vector **Q** create long-range spin-triplet correlations (LRTC) [39–42]. These superconducting correlations have a non-zero total spin projection on the quantization axis. Due to this property, exchange magnetic field do not suppress equal spin triplet pairs, which thus penetrate far into the magnetic region and thereby enhance the critical current. Our idea is to control the LRTC by changing the magnetic moments mutual orientation and in this way to control the critical current density. It was shown that in the case $\alpha = 0$ LRTC was not generated [43] like at the uniform magnetization. However, in contrast to our case, the magnetic moments considered by Champel *et al* [43] were not aligned perpendicular to the z axis, but arranged as cycloidal spin modulations in the SM interface plane. Volkov *et al* [44, 45] has shown that at the spiral vector orthogonal to the junction plane $\alpha = 90°$ the created LRTC components led to an enhancement of the critical current. However, in that approach [44] the strict assumptions on the involved wave vectors were used in contrast to our case.

Similar as described by Zyuzin *et al* [46], who analyzed a topological insulator with helical spin states our consideration will also reveal that changing the magnetization can lead to supercurrent reversals due to 0-π crossovers, which can be used to identify the states of SSV.

In section 2, we develop the model that describes the spiral reorientation in MnSi by using linearized Usadel equations. Further we use the solution of these equations as a basis to calculate the critical current density and to show how its modification can be used to discriminate SSV states, which we present in section 4. We also address the question of writing and readout of the logical states in our proposed SSV used as a memory element. Therefore, the introduced cryogenic Josephson spin valve holds a promise as a new member of the superconductor-based elements with advantages in terms of fabrication and control, together with compatibility and robustness.

2. Spiral magnetization

The considered Josephson junction is sketched in figure 1.

We have chosen the x axis perpendicular to the SM interfaces and the M layer has a thickness d_M. The spiral vector **Q** points along the z axis. The magnetic moments are oriented perpendicular to **Q** and are aligned along a spiral around **Q**.

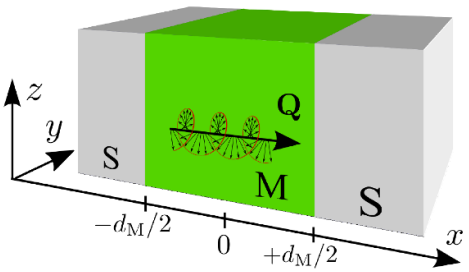

Figure 1. The Josephson junction configuration we consider. A spiral alignment of magnetic moments in the magnet M between the superconductors S, can be switched to uniform magnetization.

To determine the critical current density of this Josephson junction, we solve the linearized Usadel equations [47] which are valid in the diffusive limit. This is reasonable because low-temperature superconducting nanostructures made by sputtering are usually diffusive. The linearization step is valid close to T_c, where superconducting correlations are weak although qualitatively the results remain true in a wide range of the temperature.

We describe the superconducting correlations by using the singlet spin component f_s and the triplet spin components $\mathbf{f}_t = (f_t x, f_t y, f_t z)$ of the anomalous Green's function. The corresponding linearized Usadel equations can be written as [48, 49]

$$\begin{aligned}\left(D_M\nabla^2 - 2\,\omega\right)f_s &= 2\,\mathrm{i}\omega\,\mathbf{h}\cdot\mathbf{f}_t,\\ \left(D_M\nabla^2 - 2\,\omega\right)\mathbf{f}_t &= 2\,\mathrm{i}\omega\,\mathbf{h}f_s\end{aligned} \tag{1}$$

in the magnet and in the superconductor as

$$\begin{aligned}\left(D_s\nabla^2 - 2\,\omega\right)f_s^S &= -2\,\pi\Delta,\\ \left(D_s\nabla^2 - 2\,\omega\right)\mathbf{f}_t^S &= 0.\end{aligned} \tag{2}$$

Here, we use the diffusion coefficients D_M in the magnet and D_s in the superconductor, the superconducting order parameter Δ and the positive Matsubara frequencies $0 \leqslant \omega \equiv \omega_n = \pi T(2n+1)$, where n is an integer and T the temperature.

The magnetic vector $\mathbf{h} \equiv h[\cos(Qz), \sin(Qz), 0]$ with the value h of the exchange energy splitting is aligned along the local magnetization, which rotates in space around the spiral vector $\mathbf{Q}$, as sketched in figure 1. The spiral phase Qz describes the rotation of the magnetic moments around $\mathbf{Q}$ with a constant wave vector $Q \equiv 2\pi/\lambda$, where λ is the period of the magnetic spiral. The equation for f_{zz} separates and we can choose $f_{zz} = 0$. Since the structure which we consider is homogeneous in y direction, we only consider the differential operator $\nabla^2 = \partial^2/\partial x^2 + \partial^2/\partial z^2$. To further reduce equations (2), we follow the idea of Champel *et al* [48, 49] and perform a Fourier transformation of f_s and $\mathbf{f}_t$ along the direction z. Similar to the results of this group, we conclude that z-independent Fourier components are energetically favorable, because they represent homogeneous superconducting correlations far away from the SM interface.

Using the unitary transformation $f_\pm = (\mp f_x + i f_y)\exp(\pm iQz)$ we rewrite the Usadel equations (1) in the form

$$\begin{aligned}\left(\frac{\partial^2}{\partial x^2} - k_\omega^2\right)f_s &= \mathrm{i}k_h^2(f_- - f_+)\\ \left(\frac{\partial^2}{\partial x^2} \mp 2\,\mathrm{i}Q\frac{\partial}{\partial x} - Q^2 - k_\omega^2\right)f_\pm &= \mp 2\,\mathrm{i}\,k_h^2 f_s\end{aligned} \tag{3}$$

and the equations (2) of the superconducting parts read

$$\begin{aligned}\left(\frac{\partial^2}{\partial x^2} - k_s^2\right)f_s^S &= -2\pi\frac{\Delta}{D_S}\\ \left(\frac{\partial^2}{\partial x^2} - k_s^2\right)f_\pm^{\vec{S}} &= 0.\end{aligned} \tag{4}$$

We defined $k_\omega \equiv \sqrt{2\omega/D_M}$, $k_h \equiv \sqrt{h/D_M}$ and $k_s \equiv \sqrt{2\omega/D_s}$.

These equations are supplemented by boundary conditions according to Kupriyanov and Lukichev [50]. The derivations are transformed to $\frac{\partial}{\partial z} \to \frac{\partial}{\partial z} + \mathrm{or} - \mathrm{i}Q$ as a result of the unitary transformation we made, in contrast to works [48, 49], where $\mathbf{Q}$ was parallel to the layers and the boundary conditions remained unchanged. At $x = \pm d_M/2$ they now read

$$\begin{aligned}\frac{\partial}{\partial z}f^S{}_s &= \gamma\frac{\partial}{\partial z}f_s, & f^S{}_s &= f_s - \gamma_B\frac{\partial}{\partial z}f_s,\\ \frac{\partial}{\partial z}f^S{}_+ &= \gamma\left(\frac{\partial}{\partial z} \mp \mathrm{i}Q\right)f_+, & f^S{}_+ &= f_+ - \gamma_B\left(\frac{\partial}{\partial z} \mp \mathrm{i}Q\right)f_+,\\ \frac{\partial}{\partial z}f^S{}_- &= \gamma\left(\frac{\partial}{\partial z} \pm \mathrm{i}Q\right)f_-, & f^S{}_- &= f_- - \gamma_B\left(\frac{\partial}{\partial z} \pm \mathrm{i}Q\right)f_-.\end{aligned} \tag{5}$$

Here, we used the interface parameters $\gamma_b = R_b\sigma_M A$ and $\gamma = \sigma_M/\sigma_s$ the resistance R_b and the area A of the SM interface. The parameters σ_M and σ_s are the conductivities of the M and S material, respectively.

We use these boundary conditions to determine the solutions of the differential equations (3) and (4). We then use these solutions to derive an analytical description of the critical current density of the Josephson junction.

The growth of an MnSi thin film of a high quality may require a special substrate. It is shown that a thin normal metal or insulating interlayer in a magnetic Josephson junction changes the boundary conditions, and consequently, shifts the positions of extrema in the dependence $j_c(d_M)$ [51]. If the conductivity of this normal interlayer is similar to one of M or S metals, $j_c(d_M)$ does not change. So, if we take into account some substrate, the picture would remain qualitatively true, perhaps, with a shift along the d_M axis. This idea may be applied also to a bridge-like Josephson junction [52] based on a spiral magnet with controlling state. The control of LRTC appearance may be implemented by the same way and yield qualitatively similar results. Although the solution of related 2-dimensional problem is rather complicated and lie out of the framework of the proposed investigation.

3. Critical current density

To calculate the critical current density we consider

$$j \equiv j_c \sin\varphi = \frac{\pi T}{e\rho}\sum_{\omega>0} \mathrm{Im}\left[f_s^* \frac{\partial}{\partial x} f_s - \frac{1}{2}\left(f_-^* \frac{\partial}{\partial x} f_- + f_+^* \frac{\partial}{\partial x} f_+\right)\right]_{x=0}. \quad (6)$$

Here, φ is the phase difference between the two superconductors, e is the elementary charge and ρ describes the resistivity of the magnetic material.

We derive solutions of the Usadel equations in the magnetic layer (3) and in the superconducting layer (4) and use them for an analytical representation of the critical current density.

Using the routine described in supplementary material A we come to the critical current density

$$j_c = \frac{\pi T}{e\rho}\sum_{\omega>0}\frac{|\kappa|^2}{|||\mathcal{M}|||^2} \sum_{j,l}\mathrm{Re}\left\{k_j\left[\left(O_{j,l}^{+-} - O_{j,l}^{-+}\right)\left(U_{j,l}^{s} - U_{j,l}^{++}/2\right) - \left(X_{j,l}^{+-} - X_{j,l}^{-+}\right)\cdot\left(U_{j,l}^{s} + U_{j,l}^{+-}/2\right)\right]\right\} \quad (7)$$

where the abbreviations for $O_{j,l}^{ij}, U_{j,l}^{ij}$ and $X_{j,l}^{ij}$ are done in supplementary section.

This description of the critical current density is the basis for the logical-states which we describe below.

4. SSV states

Furthermore, we discuss the dependence of the critical current density j_c on the vector $\mathbf{Q}$ in detail, taking into account that in magnetic saturation $\mathbf{Q} = 0$, and explain how our proposed Josephson device may be used as a spin valve.

The transition-metal compounds of the MnSi family crystallize in a noncentrosymmetric cubic B20 structure that allows a linear gradient invariant [53]. This gives rise to a long-period spiral magnetic structure with wavelength $\lambda = 18$ nm. It may be switched to the magnetic saturation in low magnetic field. This device would be an analogue to the exchange coupled spin valves, the well known devices of traditional spintronics.

Further parameters for our figures are based on the publications [54, 55], where transport properties of MnSi have been studied in detail. That is, we chose the superconducting coherence length $\xi_M = 4.2$ nm, the exchange energy $h = 100$ meV for conducting electrons and the interface parameter $\gamma = 0.7$ which involves the material conductivities. From the Fermi velocities, we estimated $\gamma_B = 0.7$.

As a material for the superconducting electrodes, we chose Nb because it is commonly used in superconducting circuits. Therefore, we use the critical temperature $T_c = 9.2$ K and $\xi_s = 11$ nm from [56]. Additionally, we chose the temperature

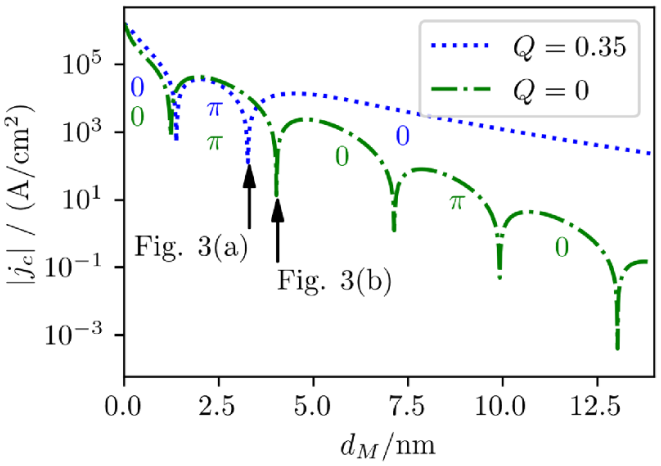

Figure 2. Critical current density $|j_c|$ as a function of d_M calculated from equation (7) in the case of in-plane spiral magnetization $Q = 0.35$ and in the homogeneous ferromagnetic case $Q = 0$, corresponding to two logical states of the proposed Josephson SSV. For two working points d_M indicated by arrows, we show the critical current density as a function of the temperature T in figure 3.

$T = 0.5\,T_c$. By using these parameters, we depicted the critical current density (7) in figure 2. It can be seen that for values larger than $d_M \approx 3.7$ nm the value of the critical current density in the spiral state $Q = 0.35\mathrm{nm}^{-1}$ is larger than in the saturation $Q = 0$. This means that for a high operating current, our proposed device can be switched between a superconducting state, which may be identified as logical state 1, and a resistivity state, which may be identified as logical state 0. Since the values of the critical current density are in the same range as those of conventional ferromagnetic Josephson junctions [57–59], our proposed device should be well compatible with other elements of Josephson low-temperature logics.

The difference in critical current density between both configurations is mainly due to long-ranged triplet correlations [23, 44, 60]. These superconducting correlations have a non-zero total spin projection on the quantization axis and can therefore penetrate far into the magnetic region and thereby enhance the critical current. They are responsible for the large critical current with a smooth decay at $d_M > 3.7$ nm in the spiral magnetic configuration. In the first working point at $d_M \approx 3.2$ nm the applied magnetic field may switch the critical current density from zero or some small value to a finite value of the order of $10\mathrm{kA\,cm}^{-2}$. It is an unusual situation where an external magnetic field does not suppress, but oppositely, restores superconductivity and enhances the Josephson current.

Our proposed device offers another interesting application at values of d_M, where the 0 state (positive critical current density) of one configuration overlaps with the π state (negative critical current density) of other configuration. This is the case e.g. in the range between $d_M \approx 3.2$ nm and $d_M \approx 4$ nm. Here, the phase shift could be related to the logical states, because it can be reversed by an external magnetic field.

In addition to choosing a specific length d_M to find a working point, where external magnetic field can be used to

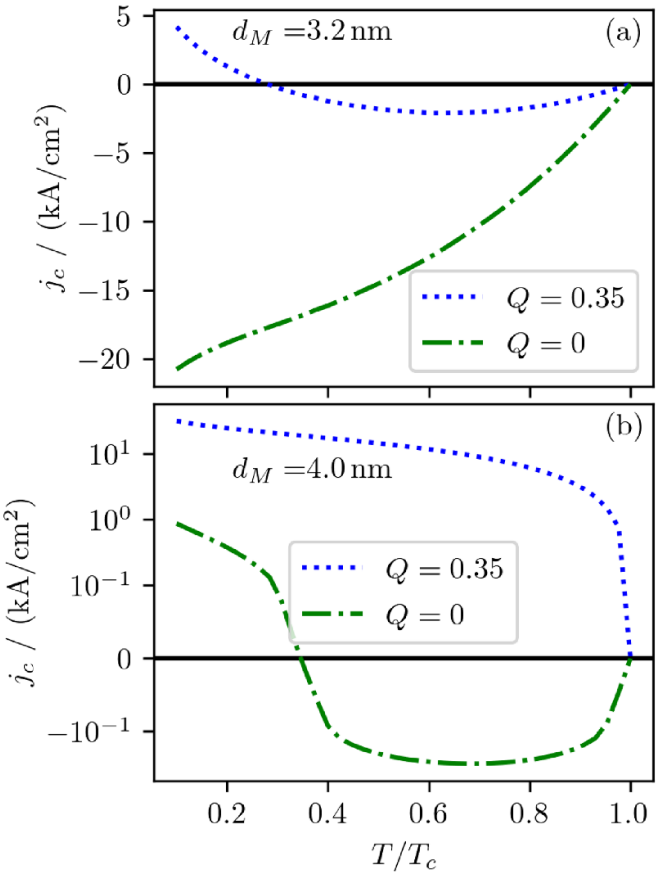

Figure 3. Critical current density j_c as a function of T for $d_M = 3.2$ nm in (a) and for $d_M = 4$ nm in (b). These figures show that one can also use the temperature T to tune our proposed device into a regime, where the critical current at the spiral magnetization has a positive sign (0 state), while the sign of the critical current in the saturation at $Q = 0$ is negative (π state).

switch between 0 and π states, one can also tune the temperature T. Although, the linear approximation is well at T around T_c, the results remain qualitatively true at lower temperatures. This can be seen in figure 3, where we depicted the critical current density j_c as a function of T for values $d_M = 3.2$ nm (a) and $d_M = 4$ nm (b), which are indicated by arrows in figure 2. In figure 3(a), a situation of opposite critical current signs can be obtained by choosing a temperature $T/T_c < 0.5$, while in figure 3(b) a temperature $T/T_c > 0.5$ leads to this situation.

The proposed mechanism of switching between the logical states could be used to change from the spiral case to a homogeneous ferromagnetic case in an external magnetic field applied in the junction plane. Such a field would fully penetrate into a weak link of a short Josephson junction. The latter situation is represented by the limit $\mathbf{Q} = 0$, which we depicted in figures 2 and 3. As can be seen in the supporting material, the critical current density at $\mathbf{Q} = 0$ behaves similar to the case $\alpha = 0$. In both cases long-range triplet correlations are absent. Similar magnetization changes have already been observed with helimagnets Ho [38, 61, 62] and Er [37], and also at the magnetization of Py [63] in superconducting devices.

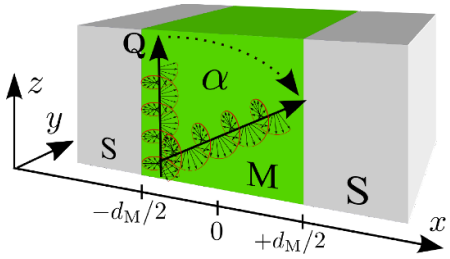

Figure 4. The Josephson junction configuration we consider. A spiral alignment of magnetic moments in the magnet M between the superconductors S, can be switched to uniform magnetization.

5. Two ground states

We propose a SSV based on a Josephson junction with a single magnetic layer (M) between the superconducting electrodes (S).

Magnetic materials with suitable properties, are itinerant cubic helimagnets of B20 family [31] like MnSi. MnSi thin films usually have magnetic anisotropy that prevents the switch of the spiral vector between a few different directions like in MnSi monocrystals [64] and the spiral vector is perpendicular to the thin-film plane. The switch between few different **Q** directions in a case of compensated anisotropy is considered below.

The plane magnetic anisotropy in SF heterostructures may be compensated in some cases [65]. We may assume that the magnetic layer of some MnSi family compound has the same properties as a crystal, i.e. has a cubic magnetic anisotropy that allows few different equivalent directions (ground states) of the spiral vector **Q**. If the vector **Q** follows crystal axes (111) and equivalent ones, like in a MnSi crystal, and one axis aligned along the junction plane along OZ, then other equivalent axis may have a maximal angle $\alpha = 0.34$ with this plane. Figure 4 presents the scheme of our junction with possible directions of the spiral.

The direction of the vector of local magnetization **h** may be expressed as

$$\mathbf{h} \equiv h \begin{pmatrix} \cos\alpha\cos\beta \\ \sin\beta \\ -\sin\alpha\cos\beta \end{pmatrix}, \quad \beta \equiv Q(z\cos\alpha + x\sin\alpha). \qquad (8)$$

It rotates in space around the spiral vector **Q**. As sketched in figure 4, the angle α characterizes a rotation of **Q** around the axis y. The angle β describes the rotation of the magnetic moments around **Q**.

The equation for f_{zz} separates and we can again choose $f_{zz} = 0$, that yields the additional condition $f_{tz} = f_{tx}\tan\alpha$. Furthermore, we use the calculation method described in sections 2 and 3. The unitary transformation has a more complicated form and is made in a way to align the quantization axes along the local magnetization in every point.

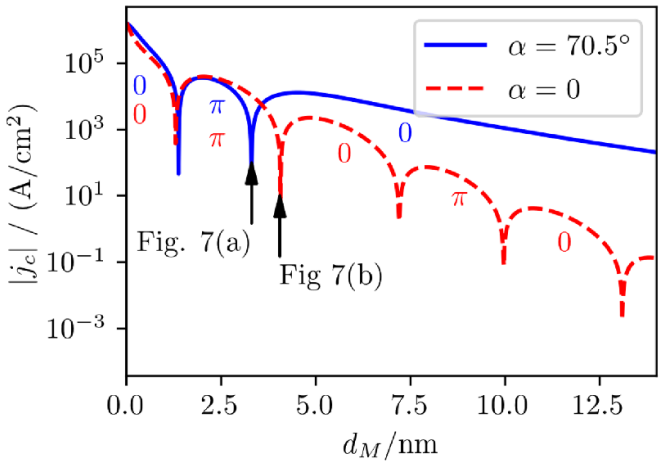

Figure 5. Critical current density $|j_c|$ as a function of d_M calculated from equation (7). As parameters, we chose $\xi_s = 11$ nm, $\xi_M = 4.2$ nm, $T_c = 9.2$ K, $T = 0.5\,T_c$, $h = 100$ meV, $\gamma = 0.7$ and $\gamma_B = 0.7$. For values larger than $d_M \approx 3.6$ nm, the critical current density in the case $\alpha = 70.5°$ is larger than in the case $\alpha = 0$. It is also larger compared to the homogeneous ferromagnetic case $Q = 0$. We propose to use the configuration of large critical current density as one logical state and one of the configurations of lower critical current density as the second logical state of a superconducting spin valve. Moreover, one may use the 0 state (positive critical current) and π state (negative critical current) for discrimination of logical states. For the values d_M indicated by two arrows, we show the critical current density as a function of the temperature T in figure 7.

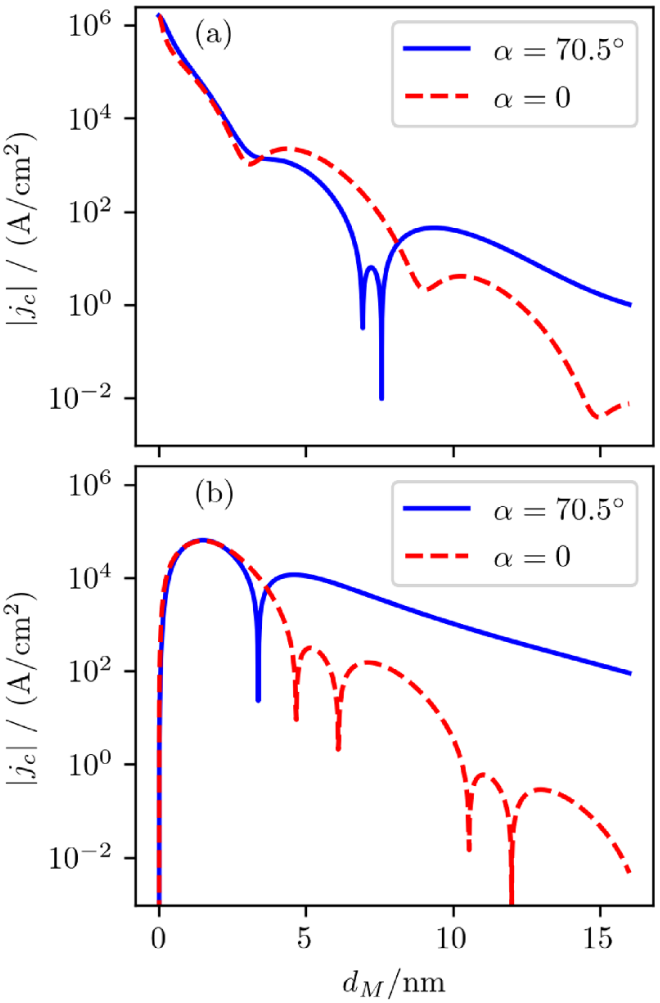

Figure 6. The singlet contribution (a) and triplet contribution (b) of the critical current density $|j_c|$ as a function of d_M calculated from equations (A15) and (A16), respectively. The significant increase of the critical current density in (b) with a change of α indicates that the source of the critical current enhancement in our proposed device are triplet correlations.

When the spiral vector **Q** inclined at the angle α to the junction plane, the additional factor $\cos\alpha$ enters in the combination $Q\cos\alpha$ in the equations (3) and (5). MnSi family compounds usually have long spiral period $\lambda = 18$ nm for MnSi crystals and **Q** has a relatively small value. We can neglect the terms with $\mathbf{Q}\sin(\alpha) \ll k_\omega, k_h$.

Here, we used the same parameters for MnSi in the calculations as in section 4.

For our analysis of the critical current density, we have chosen the angles $\alpha = 0°$ and $\alpha = 70.5°$, because in MnSi, the spiral wave vector **Q** is aligned along [111] and along equivalent directions of the cubic lattice. The angle between these directions is $\alpha = \arccos(1/3) = 70.5°$. Moreover, the transition-metal compounds of the MnSi family crystallize in a noncentrosymmetric cubic B20 structure that allows a linear gradient invariant [53]. This gives rise to a long-period spiral magnetic structure.

By using these parameters, we depicted the critical current density (7) in figure 5. It can be seen that for values larger than $d_M \approx 3.6$ nm the value of the critical current density in the configuration $\alpha = 70.5°$ is larger than in the configuration $\alpha = 0°$. This means that for a high operating current, our proposed device can be switched via α between a superconducting state, which may be identified as logical state 1 and a resisting state, which may be identified as logical state 0. Since the value of the critical current density is in the same range as that of the conventional ferromagnetic Josephson junctions [57], our proposed device should be well compatible with other logical elements based on ferromagnetic Josephson junctions.

The difference in the critical current density between both configurations, analogously to the case considered below, is due to long-ranged triplet correlations [39–42]. These superconducting correlations have a non-zero total spin projection on the quantization axis and can therefore penetrate far into the magnetic region and thereby enhance the critical current. In order to highlight this effect, we depicted in figure 6 the critical current density originating from the singlet contribution (A15) in (a) and from the triplet contribution (A16) in (b).

While the critical current density in figure 6(a) does not change significantly with α, the critical current density for $\alpha = 70.5°$ is strongly increased in figure 6(b).

In addition to choosing a specific length d_M to obtain a situation, where α can be used to switch between 0 and π states, one can also tune the temperature T. This can be seen in figure 7, where we depicted the critical current density j_c as a function of T for values $d_M = 3.2$ nm (a) and $d_M = 4$ nm (b), which are indicated by arrows in figure 5. In figure 7(a),

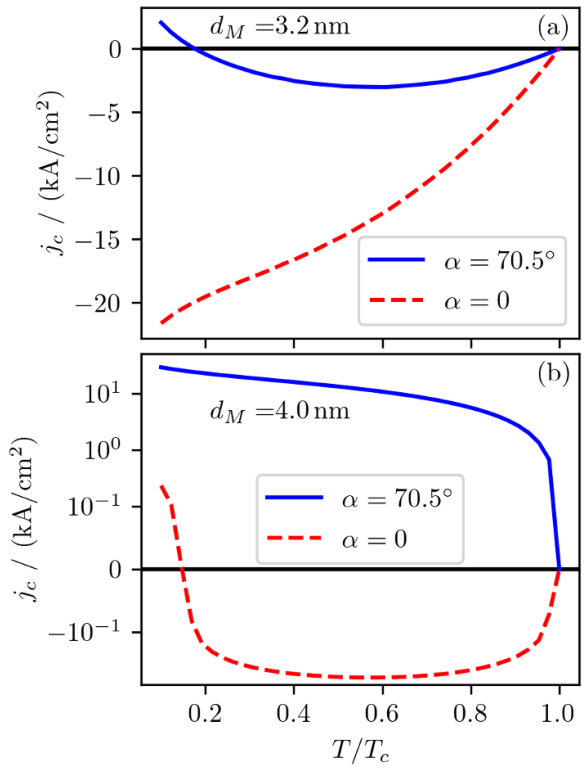

Figure 7. Critical current density j_c as a function of T for $d_M = 3.2$ nm in (a) and for $d_M = 4$ nm in (b). These figures show that one can also use the temperature T to tune our proposed device into a regime, where the critical current in the case $\alpha = 70.5°$ has a positive sign (0 state), while the sign of the critical current in the case $\alpha = 0$ and the homogenous ferromagnet case $Q = 0$ is negative (π state).

a situation of opposite critical current signs can be obtained by choosing a temperature $T/T_c < 0.5$, while in figure 3(b) a temperature $T/T_c > 0.5$ leads to this situation.

As a possible mechanism to change the angle of the spiral vector **Q**, we propose applying a short magnetic pulse along the y axis that is, perpendicular to **Q** and parallel to the superconducting layers. As a result, the magnetic field would not be suppressed by S electrodes. If the pulse length is chosen correctly, a spin precession is induced, which will rotate the magnetic moments and thereby switch the vector **Q** [32].

6. Conclusion

We have calculated the critical current density of a Josephson junction with a spiral magnet as a barrier material. The magnetic moments in this material are aligned in a spiral around a spiral vector **Q** which is usually perpendicular to the thin film plane. The amplitude of the critical current density changes and may go to zero with the saturation of magnetization. This effect is due to the change of long ranged triplet correlations.

We propose to use this Josephson junction as a spin valve, where the logical states are defined by spiral and uniform magnetization. Additionally, supercurrent reversals due to 0-π crossovers can be used to identify the logical states. This crossover may be reached at other thicknesses of the M layer. The logical states which belong to the rotation of vector **Q** towards the plane of the superconducting interface were also considered (see supplementary material B).

In summary, the single-barrier design, stable ground states and compatibility with other Josephson devices make our proposed device a promising candidate for a novel cryogenic Josephson spin valve.

Data availability statement

The data that support the findings of this study are available upon reasonable request from the authors.

Acknowledgments

We thank Dr V Dyadkin, ESRF, Grenoble, France, and Prof. E G Ekomasov, BSPU, Ufa, Russia for fruitful discussions. This work was financially supported by the Ministry of Science and Higher Education of the Russian Federation, Megagrant Project No. 075-15-2019-1934 in part of the scientific problem formulation and analysis. The discussion of spiral to uniform magnetization switch was financially supported by RFBR according to the research Project No. 19-02-00316. The discussion of two ground states was financially supported by the program Mirror Labs of HSE University for support of inter-Russian cooperation.

Appendix A. Critical current calculation

Starting from the expression of the current density (6), we insert here the general solutions

$$f_s(x) = \sum_{j=0}^{2} A_j u_{s,j} e^{-k_j x} + B_j v_{s,j} e^{+k_j x},$$
$$f_+(x) = \sum_{j=0}^{2} A_j u_{+,j} e^{-k_j x} + B_j v_{+,j} e^{+k_j x},$$
$$f_-(x) = \sum_{j=0}^{2} A_j u_{-,j} e^{-k_j x} + B_j v_{-,j} e^{+k_j x} \quad \text{(A9)}$$

of the differential equations in the magnetic layer (3). This leads us to the singlet contribution

$$\left[f_s{}^* \frac{\partial}{\partial x} f_s\right]_{x=0} = \sum_{j,l=0}^{2} \left(k_j u_{s,j} u^*_{s,l}\right) \left(-A_j A_l^* + B_j B_l^* + + B_j A_l^* - A_j B_l^*\right) \quad \text{(A10)}$$

and the triplet contribution

$$\left[{f_+}^*\frac{\partial}{\partial x}f_+ + {f_-}^*\frac{\partial}{\partial x}f_-\right]_{x=0} = \sum_{j,l=0}^{2}\left(-A_j u_{+,j}k_j - B_j u_{-,j}k_j\right)\left(A_l^* u_{+,l}^* - B_l^* u_{-,l}^*\right) + \left(-A_j u_{-,j}k_j - B_j u_{+,j}k_j\right)\left(A_l^* u_{-,l}^* - B_l^* u_{+,l}^*\right). \quad \text{(A11)}$$

For the a complete description of the current density, the three parameters k_j, the vectors $\mathbf{u}_j \equiv (u_{\mathrm{s},j}, u_{+,j}, u_{-,j})^{\mathrm{T}}$ and $\mathbf{v} \equiv (v_{\mathrm{s},j}, v_{+,j}, v_{-,j})^{\mathrm{T}}$ and the six constants A_j and B_j are required.

In order to determine the parameters k_j, we insert the solutions (A9) into the differential equations (3). Solving the corresponding characteristic equation leads us to the values k_j. For MnSi we take $k_{\mathrm{h}} \approx 0.7\ \mathrm{nm}^{-1}$, $Q \approx 0.35\ \mathrm{nm}^{-1}$ and $k_\omega \approx 0.14\ \mathrm{nm}^{-1}$ [54, 55]. By using k_j together with the solutions (A9) in the differential equation (3), we obtain the vectors $\mathbf{u}_j$ and $\mathbf{v}_j$. In the limit $k_h^2 \gg Q^2, k_\omega^2$ our solution coincide with one in the work [44].

To determine the six constants A_j and B_j, we make use of the boundary conditions (5). First, we insert the solutions $f_{\mathrm{s},\pm}^{\mathrm{S}-}$ for $x \leqslant -d_{\mathrm{M}}/2$ and the solutions $f_{\mathrm{s},\pm}^{\mathrm{S}+}$ for $x \geqslant d_{\mathrm{M}}/2$ of the Usadel equations (4) in the superconductor. By assuming an exponential decay of the triplet correlations in the superconducting material, we write them as

$$\begin{aligned} f_{\mathrm{s}}^{\mathrm{S}\pm}(x) &= \frac{\pi}{\omega}\Delta \mathrm{e}^{\pm \mathrm{i}\varphi/2} + C_{\mathrm{s}}^{\pm}\mathrm{e}^{(\mp x + d_{\mathrm{M}}/2)k_{\mathrm{s}}}, \\ f_{+}^{\mathrm{S}\pm}(x) &= C_{+}^{\pm}\mathrm{e}^{(\mp x + d_{\mathrm{M}}/2)k_{\mathrm{s}}}, \\ f_{-}^{\mathrm{S}\pm}(x) &= C_{-}^{\pm}\mathrm{e}^{(\mp x + d_{\mathrm{M}}/2)k_{\mathrm{s}}}, \end{aligned} \quad \text{(A12)}$$

where we introduced the six constants $C_{\mathrm{s},\pm}^{\pm}$.

By using the S-layer solutions (A12) and M-layer solutions (A9) in the boundary conditions (5) at $-d_{\mathrm{M}}/2$ and $+d_{\mathrm{M}}/2$, we obtain 12 equations with 12 constants. We eliminate the constants $C_{\mathrm{s},\pm}^{\pm}$ in order to reduce the system to

$$\mathcal{M}\begin{pmatrix} A_0 \\ A_1 \\ A_2 \\ B_0 \\ B_1 \\ B_2 \end{pmatrix} = \begin{pmatrix} \kappa \mathrm{e}^{+\mathrm{i}\varphi/2} \\ 0 \\ 0 \\ \kappa \mathrm{e}^{-\mathrm{i}\varphi/2} \\ 0 \\ 0 \end{pmatrix}, \quad \text{(A13)}$$

where $\mathcal{M}$ is a 6×6 matrix and we defined $\kappa \equiv \pi\Delta/\omega$. The solution of the system (A13) can be written as as

$$\begin{aligned} A_j &= \kappa \frac{a_j^+ \mathrm{e}^{+\mathrm{i}\varphi/2} + a_j^- \mathrm{e}^{-\mathrm{i}\varphi/2}}{\|\mathcal{M}\|}, \\ B_j &= \kappa \frac{b_j^+ \mathrm{e}^{+\mathrm{i}\varphi/2} + b_j^- \mathrm{e}^{-\mathrm{i}\varphi/2}}{\|\mathcal{M}\|}, \end{aligned} \quad \text{(A14)}$$

where $a_j^{\pm}$ and $b_j^{\pm}$ are the coefficients according to Cramer's rule and $\|\mathcal{M}\|$ is the determinant of the matrix $\mathcal{M}$.

We insert the constants (A14) into the singlet part (A10) to obtain

$$[{f_{\mathrm{s}}}^*\partial_z f_{\mathrm{s}}]_{z=0} = \frac{|\kappa|^2}{|\|\mathcal{M}\||^2}\sum_{j,l} k_j \times \left[\mathrm{i}\sin\varphi\left(O_{j,l}^{+-} - O_{j,l}^{-+} - X_{j,l}^{+-} + X_{j,l}^{-+}\right)\right]U_{j,l}^{0} \quad \text{(A15)}$$

and into the triplet part (A11) to obtain

$$[{f_+}^*\partial_z f_+ + {f_-}^*\partial_z f_-]_{z=0} = \frac{|\kappa|^2}{|\|\mathcal{M}\||^2}\sum_{j,l} k_j \left\{\mathrm{i}\sin\varphi\left[\left(O_{j,l}^{+-} - O_{j,l}^{-+}\right)U_{j,l}^{++} + \left(X_{j,l}^{+-} - X_{j,l}^{-+}\right)U_{j,l}^{+-}\right]\right\}. \quad \text{(A16)}$$

Here we used abbreviations

$$\begin{aligned} X_{j,l}^{m,n} &\equiv a_j^m b_l^{n*} - b_j^m a_l^{n*} \\ O_{j,l}^{m,n} &\equiv b_j^m b_l^{n*} - a_j^m a_l^{n*} \\ U_{j,l}^{m,n} &\equiv u_{m,j}{u_{n,l}}^* + u_{-m,j}{u_{-n,l}}^* \\ U_{j,l}^{\mathrm{s}} &\equiv u_{\mathrm{s},j}{u_{\mathrm{s},l}}^*. \end{aligned} \quad \text{(A17)}$$

By inserting the singlet contribution (A15) and the triplet contribution (A16) into equation (6), we obtain the critical current density (7).

ORCID iDs

N G Pugach https://orcid.org/0000-0003-4017-1667
D M Heim https://orcid.org/0000-0002-2107-9729
D V Seleznev https://orcid.org/0000-0002-8249-2496
A I Chernov https://orcid.org/0000-0002-6492-9068
D Menzel https://orcid.org/0000-0001-6455-3868

References

[1] Ball P 2012 Feeling the heat *Nature* **492** 174
[2] Service R F 2012 What it'll take to go exascale *Science* **335** 394–6
[3] Brock D C 2016 The nsa's frozen dream *IEEE Spectr.* **53** 54–60
[4] Klenov N, Kornev V, Vedyayev A, Ryzhanova N, Pugach N and Rumyantseva T 2010 Josephson junctions with nonsinusoidal current-phase relations based on heterostructures with a ferromagnetic spacer and their applications *Phys. Solid State* **52** 2246
[5] Manheimer M 2015 Cryogenic computing complexity program: phase 1 introduction *IEEE Trans. Appl. Supercond.* **25** 1–4
[6] Holmes D S *et al* 2019 *Cryogenic Electronics and Quantum Information Processing (2018 update)* (New York: IEEE) pp 34–42
[7] Soloviev I I, Klenov N V, Bakurskiy S V, Kupriyanov M Y, Gudkov A L and Sidorenko A S 2017 After Moore's technologies: operation principles of a superconductor alternative *Beilstein J. Nanotechnol.* **8** 2689–710

[8] Polonsky S V, Kirichenko A F, Semenov V K and Likharev K K 1995 Rapid single flux quantum random access memory *IEEE Trans. Appl. Supercond.* **5** 3000–5

[9] Nagasawa S, Numata H, Hashimoto Y and Tahara S 1999 High-frequency clock operation of Josephson 256-word/spl times/16-bit RAMs *IEEE Trans. Appl. Supercond.* **9** 3708–13

[10] Liu Q, Duzer T V, Meng X, Whiteley S R, Fujiwara K, Tomida T, Tokuda K and Yoshikawa N 2005 Simulation and measurements on a 64-kbit hybrid Josephson-CMOS memory *IEEE Trans. Appl. Supercond.* **15** 415–18

[11] Tanaka M, Suzuki M, Konno G, Ito Y, Fujimaki A and Yoshikawa N 2017 Josephson-CMOS hybrid memory with nanocryotrons *IEEE Trans. Appl. Supercond.* **27** 1800904

[12] Ustinov A V and Kaplunenko V K 2003 Rapid single-flux quantum logic using -shifters *J. Appl. Phys.* **94** 5405

[13] Ortlepp T *et al* 2006 Flip-flopping fractional flux quanta *Science* **312** 1495

[14] Bakurskiy S V *et al* 2017 Current-phase relations in SIsFS junctions in the vicinity of 0-π transition *Phys. Rev.* B **95** 09452

[15] Yamanashi Y, Nakaishi S, Sugiyama A, Takeuchi N and Yoshikawa N 2018 Design methodology of single-flux-quantum flip-flops composed of both 0- and π-shifted Josephson junctions *Supercond. Sci. Technol.* **31** 105003

[16] Soloviev I I *et al* 2021 Superconducting circuits without inductors based on bistable Josephson junctions *Phys. Rev. Appl.* **16** 014052

[17] Goldobin E, Sickinger H, Weides M, Ruppelt N, Kohlstedt H, Kleiner R and Koelle D 2013 Memory cell based on a φ Josephson junction *Appl. Phys. Lett.* **102** 242602

[18] Pugach N G, Goldobin E, Kleiner R and Koelle D 2010 Method for reliable realization of a φ Josephson junction *Phys. Rev.* B **81** 104513

[19] Heim D M, Pugach N G, Kupriyanov M Y, Goldobin E, Koelle D and Kleiner R 2013 Ferromagnetic planar Josephson junction with transparent interfaces: a junction proposal *J. Phys.: Condens. Matter.* **25** 215701

[20] Vernik I V, Bol'ginov V V, Bakurskiy S V, Golubov A A, Kupriyanov M Y, Ryazanov V V and Mukhanov O A 2013 Magnetic Josephson junctions with superconducting interlayer for cryogenic memory *IEEE Trans. Appl. Supercond.* **23** 1701208

[21] Zdravkov V I *et al* 2013 Memory effect and triplet pairing generation in the superconducting exchange biased $Co/CoO_x/Cu_{41}Ni_{59}/Nb/Cu_{41}Ni_{59}$ layered heterostructure *Appl. Phys. Lett.* **103** 062604

[22] Niedzielski B M, Diesch S G, Gingrich E C, Wang Y, Loloee R, Pratt W P and Birge N O 2014 Use of Pd-Fe and Ni-Fe-Nb as soft magnetic layers in ferromagnetic Josephson junctions for nonvolatile cryogenic memory *IEEE Trans. Appl. Supercond.* **24** 1800307

[23] Pugach N G, Safonchik M, Champel T, Zhitomirsky M E, Lahderanta E, Eschrig M and Lacroix C 2017 Superconducting spin valves controlled by spiral re-orientation in MnSi *Appl. Phys. Lett.* **111** 162601

[24] Baek B, Rippard W H, Benz S P, Russek S E and Dresselhaus P D 2014 Hybrid superconducting-magnetic memory device using competing order parameters *Nat. Commun.* **5** 3888

[25] Vedyayev A, Lacroix C, Pugach N and Ryzhanova N 2005 Spin-valve magnetic sandwich in a Josephson junction *Europhys. Lett.* **71** 679–85

[26] Vedyayev A, Ryzhanova N and Pugach N 2006 Critical current oscillations in S/F heterostructures in the presence of sâd scattering *J. Magn. Magn. Mater.* **305** 53–6

[27] Ye L, Wolf G, Pinna D, Chaves-O'Flynn G D and Kent A D 2015 State diagram of an orthogonal spin transfer spin valve device *J. Appl. Phys.* **117** 193902

[28] Golod T, Iovan A and Krasnov V M 2015 Single Abrikosov vortices as quantized information bits *Nat. Commun.* **6** 8628

[29] Bakurskiy S V, Klenov N V, Soloviev I I, Pugach N G, Kupriyanov M Y and Golubov A A 2018 Protected 0-π states in SIsFS junctions for Josephson memory and logic *Appl. Phys. Lett.* **113** 082602

[30] Murphy A, Averin D V and Bezryadin A 2017 Nanoscale superconducting memory based on the kinetic inductance of asymmetric nanowire loops *New J. Phys.* **19** 063015

[31] Grigoriev S V, Maleyev S V, Okorokov A I, Chetverikov Y O, Böni P, Georgii R, Lamago D, Eckerlebe H and Pranzas K 2006 Magnetic structure of MnSi under an applied field probed by polarized small-angle neutron scattering *Phys. Rev.* B **74** 214414

[32] Gusev N A, Dgheparov D I, Pugach N G and Belotelov V I 2021 Magnonic control of the superconducting spin valve by magnetization reorientation in a helimagnet *Appl. Phys. Lett.* **118** 232601

[33] Shirane G, Cowley R, Majkrzak C, Sokoloff J B, Pagonis B, Perry C H and Ishikawa Y 1983 Spiral magnetic correlation in cubic MnSi *Phys. Rev.* B **28** 6251–5

[34] Grigoriev S V, Maleyev S V, Dyadkin V A, Menzel D, Schoenes J and Eckerlebe H 2007 Principal interactions in the magnetic system $Fe_{1-x}Co_xSi$: magnetic structure and critical temperature by neutron diffraction and squid measurements *Phys. Rev.* B **76** 092407

[35] Neubauer A, Pfleiderer C, Binz B, Rosch A, Ritz R, Niklowitz P G and Böni P 2009 Topological Hall effect in the a phase of MnSi *Phys. Rev. Lett.* **102** 186602

[36] Fujishiro Y *et al* 2019 Topological transitions among skyrmion- and hedgehog-lattice states in cubic chiral magnets *Nat. Commun.* **10** 1059

[37] Satchell N, Witt J D S, Flokstra M G, Lee S L, Cooper J F K, Kinane C J, Langridge S and Burnell G 2017 Control of superconductivity with a single ferromagnetic layer in niobium/erbium bilayers *Phys. Rev. Appl.* **7** 044031

[38] Chiodi F *et al* 2013 Supra-oscillatory critical temperature dependence of Nb-Ho bilayers *Europhys. Lett.* **101** 37002

[39] Bergeret F S, Volkov A F and Efetov K B 2001 Josephson current in superconductor-ferromagnet structures with a nonhomogeneous magnetization *Phys. Rev.* B **64** 134506

[40] Kadigrobov A, Shekhter R I and Jonson M 2001 Quantum spin fluctuations as a source of long-range proximity effects in diffusive ferromagnet-super conductor structures *Europhys. Lett.* **54** 394

[41] Keizer R, Goennenwein S, Klapwijk T, Miao G, Xiao G and Gupta A 2006 A spin triplet supercurrent through the half-metallic ferromagnetCrO_2 *Nature* **439** 825–8

[42] Khaire T S, Khasawneh M A, Pratt W P and Birge N O 2010 Observation of spin-triplet superconductivity in Co-based Josephson junctions *Phys. Rev. Lett.* **104** 137002

[43] Champel T, Löfwander T and Eschrig M 2008 0-π transitions in a superconductor/chiral ferromagnet/superconductor junction induced by a homogeneous cycloidal spiral *Phys. Rev. Lett.* **100** 077003

[44] Volkov A F, Anishchanka A and Efetov K B 2006 Odd triplet superconductivity in a superconductor/ferromagnet system with a spiral magnetic structure *Phys. Rev.* B **73** 104412

[45] Alidoust M and Halterman K 2015 Proximity induced vortices and long-range triplet supercurrents in ferromagnetic Josephson junctions and spin valves *J. Appl. Phys.* **117** 123906

[46] Zyuzin A, Alidoust M, and Loss D 2016 Josephson junction through a disordered topological insulator with helical magnetization *Phys. Rev.* B **93** 214502

[47] Usadel K D 1970 Generalized diffusion equation for superconducting alloys *Phys. Rev. Lett.* **25** 507–9
[48] Champel T and Eschrig M 2005a Switching superconductivity in superconductor/ferromagnet bilayers by multiple-domain structures *Phys. Rev.* B **71** 220506
[49] Champel T and Eschrig M 2005b Effect of an inhomogeneous exchange field on the proximity effect in disordered superconductor-ferromagnet hybrid structures *Phys. Rev.* B **72** 054523
[50] Kuprianov M Y and Lukichev V F 1988 Effect of boundary transparency the critical current in dirty SS's structures *Zh. Eksp. Teor. Fiz.* **94** 139-49 [Sov. Phys. JETP 67, 1163 (1988)]
[51] Heim D M, Pugach N G, Kupriyanov M Y, Goldobin E, Koelle D, Kleiner R, Ruppelt N, Weides M and Kohlstedt H 2015 The effect of normal and insulating layers on 0-π transitions in Josephson junctions with a ferromagnetic barrier *New J. Phys.* **17** 113022
[52] Karminskaya T Y, Golubov A A, Kupriyanov M Y and Sidorenko A S 2010 Josephson effect in superconductor/ferromagnet structures with a complex weak-link region *Phys. Rev.* B **81** 214518
[53] Bak P and Jensen M H 1980 Theory of helical magnetic structures and phase transitions in MnSi and FeGe *J. Phys. C: Solid State Phys.* **13** L881
[54] Lee M, Onose Y, Tokura Y and Ong N P 2007 Hidden constant in the anomalous Hall effect of high-purity magnet MnSi *Phys. Rev.* B **75** 172403
[55] Jonietz F *et al* 2010 Spin transfer torques in MnSi at ultralow current densities *Science* **330** 1648–51
[56] Flokstra M G *et al* 2016 Remotely induced magnetism in a normal metal using a superconducting spin-valve *Nat. Phys.* **12** 57–61
[57] Oboznov V A, Bol'ginov V V, Feofanov A K, Ryazanov V V and Buzdin A I 2006 Thickness dependence of the Josephson ground states of superconductor-ferromagnet-superconductor junctions *Phys. Rev. Lett.* **96** 197003
[58] Khaydukov Y N *et al* 2018 Magnetic and superconducting phase diagram of Nb/Gd/Nb trilayers *Phys. Rev.* B **97** 144511
[59] Ozaeta A, Vasenko A S, Hekking F W J and Bergeret F S 2012 Andreev current enhancement and subgap conductance of superconducting *SFN* hybrid structures in the presence of a small spin-splitting magnetic field *Phys. Rev.* B **86** 060509
[60] Pugach N G and Safonchik M O 2018 Increase in the critical temperature of the superconducting transition of a hybrid structure upon the magnetization of spiral antiferromagnets *JETP Lett.* **107** 302306
[61] Gu Y, Halász G B, Robinson J W A and Blamire M G 2015 Large superconducting spin valve effect and ultrasmall exchange splitting in epitaxial rare-earth-niobium trilayers *Phys. Rev. Lett.* **115** 067201
[62] Bernardo A Di, Diesch S, Gu Y, Linder J, Divitini G, Ducati C, Scheer E, Blamire M G and Robinson J W A 2015 Signature of magnetic-dependent gapless odd frequency states at superconductor/ferromagnet interfaces *Nat. Commun.* **6** 8053
[63] Cirillo C, Voltan S, Ilyina E A, HernÃndez J M, GarcÃa-Santiago A, Aarts J and Attanasio C 2017 Long-range proximity effect in Nb-based heterostructures induced by a magnetically inhomogeneous permalloy layer *New J. Phys.* **19** 023037
[64] Menzel D, Engelke J, Reimann T and Süllow S 2013 Enhanced critical fields in MnSi thin films *J. Kor. Phys. Soc.* **62** 1580
[65] Sickinger H, Lipman A, Weides M, Mints R G, Kohlstedt H, Koelle D, Kleiner R and Goldobin E 2012 Experimental evidence of a φJosephson junction *Phys. Rev. Lett* **109** 107002